

## Analysis of Crack Tip Stress Using Compactly Supported Meshless Method

T. S. Li<sup>1</sup>, S. M. Wong<sup>1</sup>, K. S. Chan<sup>1</sup>

### Summary

In this paper, a mesh-free algorithm is developed for the analysis of crack tip stress in isotropic materials. The proposed algorithm is derived from a class of continuously differentiable and positive definite compactly supported radial basis functions (CSRBFs). Two classical crack tip problems are solved as examples. The stress intensity factors are analyzed to exhibit the performance of the proposed method.

### Introduction to Compactly Supported Meshless Functions

This paper introduces a meshless algorithm derived from a class of compactly supported radial basis functions (CSRBFs) for solving the governing partial differential equations of plane elasticity problems involving single crack. CSRBFs have the advantage of a simple mathematical formulation and truly mesh free property. The continuously differentiable, positive definite and integrable features of CSRBFs can also be a great benefit in solving higher order partial differential equations with complicated boundaries.

CSRBFs were firstly introduced by Wu [1] and later expanded by Wendland [2] in the mid 1990s. The principle idea of CSRBFs is to use a polynomial as a function of Euclidean distance  $r$  with support on  $[0, 1]$  and vanish on  $[1, \infty]$ . The basic definition of the CSRBF  $\phi_{l,k}(r)$  have the form

$$\phi_{l,k}(r) = [1 - r]_+^n p(r), \text{ for } k \geq 1 \tag{1}$$

subject to following conditions

$$[1 - r]_+^n = \begin{cases} (1 - r)^n & \text{if } 0 \leq r < 1; \\ 0 & \text{if } r \geq 1, \end{cases}$$

where  $p(r)$  is a prescribed polynomial,  $r = \| \mathbf{x} - \mathbf{x}_j \|$ ,  $j = 1, 2, \dots, N$  is the Euclidean distance and  $\mathbf{x}, \mathbf{x}_j \in \mathbf{R}^d$ . The index  $l$  in (1) is the dimension number and  $2k$  is the smoothness of the function. For small number of  $k = 0, 1, 2, 3$ , Wendland's CSRBFs can be formulated explicitly in the following expressions

$$\left. \begin{aligned} \phi_{l,0}(r) &\doteq [1 - r]_+^l, \\ \phi_{l,1}(r) &\doteq [1 - r]_+^{l+1} [(l + 1)r + 1], \\ \phi_{l,2}(r) &\doteq [1 - r]_+^{l+2} [(l^2 + 4l + 3)r^2 + (3l + 6)r + 3], \\ \phi_{l,3}(r) &\doteq [1 - r]_+^{l+3} [(l^3 + 9l^2 + 23l + 15)r^3 \\ &\quad + (6l^2 + 36l + 45)r^2 + (15l + 45)r + 15]. \end{aligned} \right\} \tag{2}$$

The value  $l$  is determined by  $\lfloor \frac{d}{2} \rfloor + k + 1$ , where  $d$  is the dimension number.

---

<sup>1</sup>School of Science and Technology, the Open University of Hong Kong, China

Let  $f(\mathbf{x}) : \mathbf{R} \rightarrow \mathbf{R}$  be a real-valued function and let  $\{\mathbf{x}_j : j = 1, 2, \dots, N\} \in \mathbf{R}^d$  be  $N$  distinct points. Let  $\phi_{l,k}(r_j)$  be a positive definite CSRBFs, where  $r_j = \|\mathbf{x} - \mathbf{x}_j\|$  is the Euclidean distance between  $\mathbf{x}$  and  $\mathbf{x}_j$ . We can scale a basis function with compact support on  $[0, \delta]$  by replacing  $r_i$  with  $r_i/\delta_i$  where  $\delta_i > 0$ . With a scaling factor  $\delta_i$  the compactly supported approximation function  $s(\mathbf{x})$  to  $f(\mathbf{x})$  can be written as

$$s(\mathbf{x}) = \sum_{j=1}^N \alpha_j^n \phi_{l,k} \left( \frac{r_j}{\delta_j} \right), \tag{3}$$

where  $\delta_j$  can be variable or constant for different node points depends on the nature of the problem. In general, the smaller the value of  $\delta_i$ , the higher percentage of zero entries. However, this would also be resulted in lower accuracy. The Error bound for CSRBFs approximation of  $f \in H^s(\mathbf{R}^d)$  can be found in [3].

### Governing Equations of Single Crack Models

To illustrate the application of CSRBFs, two classical crack problems subject to tensions are considered.

**Model 1: Single-edge crack** problem contains a single edged-crack along the negative  $x$ -axis and its crack tip occurs at the origin over a square plate as depicted in Figure 1(a). The solution of the problem has been found to be anti-symmetric. This leads to have the transformation property that requires only to solve the upper-half of the square plate defined on  $\Omega = \{(x, y), -\frac{a}{2} \leq x \leq \frac{a}{2}, 0 \leq y \leq \frac{a}{2}\}$

**Model 2: Centre crack** problem contains a single crack in the centre of a square plate as illustrated in Figure 1(b). This problem satisfies the symmetry property, so only the quarter region of the plate defined on  $\Omega = \{(x, y), 0 \leq x \leq \frac{a}{2}, 0 \leq y \leq \frac{a}{2}\}$  is considered.

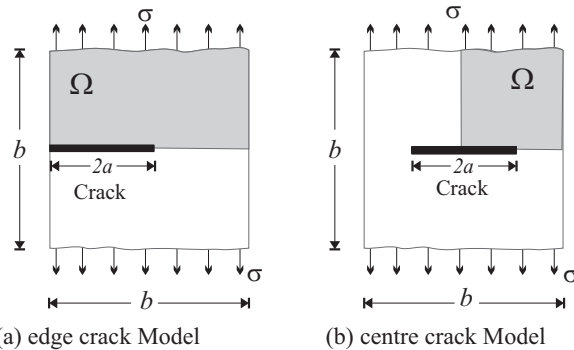


Figure 1: Two examples of mode I crack tip problems

These two models involve the following set of equilibrium equations resolved into the  $x$  and  $y$  directions

$$\frac{\partial \sigma_x}{\partial x} + \frac{\partial \tau_{xy}}{\partial y} = 0, \text{ and } \frac{\partial \tau_{xy}}{\partial x} + \frac{\partial \sigma_y}{\partial y} = 0,$$

subject to the essential and natural boundary conditions over the solved domain  $\Omega$ . The corresponding function of stresses,  $\sigma_x$ ,  $\sigma_y$  and shear stress,  $\tau_{xy}$  are defined by

$$\sigma_x = \frac{E}{(1-\nu^2)} (\epsilon_x + \nu\epsilon_y); \sigma_y = \frac{E}{(1-\nu^2)} (\epsilon_y + \nu\epsilon_x); \tau_{xy} = \frac{E}{2(1+\nu)} (\gamma_{xy})$$

where  $\epsilon_x = \partial u/\partial x$ ,  $\epsilon_y = \partial v/\partial y$  are the strains in  $x$  and  $y$  directions respectively,  $\gamma_{xy} = \partial v/\partial x + \partial u/\partial y$  is the shear strain,  $\nu$  is the Poisson's ratio and  $E$  is the Young's modulus,  $u$  and  $v$  being displacements in  $x$  and  $y$  directions respectively. According to these equations, the governing displacements equations in  $\Omega \setminus \partial\Omega \subset \mathbf{R}^2$ , can be modelled by the following system of equations

$$\frac{1}{(1-\nu)} \frac{\partial^2 u}{\partial x^2} + \frac{(1+\nu)}{2(1-\nu)} \frac{\partial^2 v}{\partial x \partial y} + \frac{1}{2} \frac{\partial^2 u}{\partial y^2} = 0; \tag{4}$$

$$\frac{1}{(1-\nu)} \frac{\partial^2 v}{\partial y^2} + \frac{(1+\nu)}{2(1-\nu)} \frac{\partial^2 u}{\partial x \partial y} + \frac{1}{2} \frac{\partial^2 v}{\partial x^2} = 0. \tag{5}$$

The local analytic solution of the displacements  $u$  and  $v$  in the vicinity of the crack tip can be modelled by a series expansions in polar coordinates  $(r, \theta)$  about the crack tip. According to the results presented by Nairn [4], the analytic solution of the tangential displacements with respect to  $r$  and  $\theta$  are given respectively by

$$u_r = \frac{1}{2E} \sum_{n=1}^{\infty} r^{\frac{n}{2}} \left\{ \begin{array}{l} C_{1n} [\gamma_1 \cos(\frac{n-2}{2}\theta) + \gamma_2 \cos(\frac{n+2}{2}\theta)] + \\ C_{2n} [\gamma_1 \sin(\frac{n-2}{2}\theta) + \gamma_3 \sin(\frac{n+2}{2}\theta)] \end{array} \right\}, \tag{6}$$

$$u_\theta = \frac{1}{2E} \sum_{n=1}^{\infty} r^{\frac{n}{2}} \left\{ \begin{array}{l} C_{1n} [\gamma_4 \sin(\frac{n-2}{2}\theta) - \gamma_2 \sin(\frac{n+2}{2}\theta)] + \\ C_{2n} [-\gamma_4 \cos(\frac{n-2}{2}\theta) + \gamma_3 \cos(\frac{n+2}{2}\theta)] \end{array} \right\}. \tag{7}$$

where  $C_{1n}$  and  $C_{2n}$  are the expansion coefficients to be determined. The terms  $\gamma_1$ ,  $\gamma_2$ ,  $\gamma_3$  and  $\gamma_4$  are defined by

$$\begin{aligned} \gamma_1 &= 6 - n - \nu(n+2), & \gamma_2 &= (n+2 - 4I_n)(1+\nu), \\ \gamma_3 &= (n-2 + 4I_n)(1+\nu), & \gamma_4 &= n+6 + \nu(n-2), \end{aligned}$$

subject to the following conditions  $I_n = n \bmod 2 = \begin{cases} 0 & \text{when } n \text{ is even;} \\ 1 & \text{when } n \text{ is odd.} \end{cases}$

The series solution automatically satisfies the equilibrium condition given by equations (4) and (5).

### Computational Algorithm and Results

To handle the boundary singularity in the neighbourhood of the crack tip, we adopt the overlapping decomposition technique. The solved domain is divided into two overlapping subdomains  $\Omega_1$  and  $\Omega_2$  such that  $\Omega = \Omega_1 \cup \Omega_2$  as depicted in Figure 2. The subdomain  $\Omega_2$  as shown in Figure 2(b) is the open upper-half rectangle, which covers the neighbourhood of the crack tip. In this study, the numerical solutions in  $\Omega_1$  is calculated by using

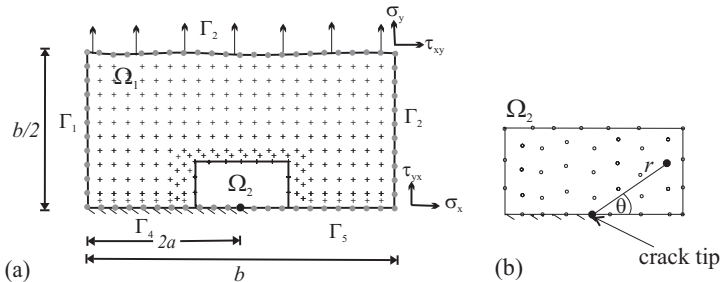


Figure 2: (a) The collocation points in  $\Omega_1$ , (b) the collocation points in  $\Omega_2$ .

Wendland's CSRBFs, while the series expansions (6) and (7) are used to approximate the displacements in  $\Omega_2$ . In order to ensure the smoothness across the two regions  $\Omega_1$  and  $\Omega_2$ , we include some nodal points in  $\Omega_2$  when we formulate the CSRBFs method for the sub-domain  $\Omega_1$ . Similarly, some of the nodal points in  $\Omega_1$  are also included in the formulation of the series expansion method for  $\Omega_2$ .

Let  $X_1 = \{\mathbf{x}_1, \mathbf{x}_2, \dots, \mathbf{x}_{N_1}\} \subset \mathbf{R}^2$  be a set of distinct interior points that are selected to coincide with the collocation points in  $\Omega_1 \setminus \partial\Omega$ ,  $X_2 = \{\mathbf{x}_{(N_1+1)}, \dots, \mathbf{x}_{(N_1+N_2)}\}$  in  $\partial\Omega$  be the boundary points, and  $X_3 = \{\mathbf{x}_{(N_1+N_2+1)}, \dots, \mathbf{x}_{(N_1+N_2+N_3)}\}$  be a small set of nodal points in  $\Omega_1 \cap \Omega_2$ . Let  $N$  be the total number of collocation points such that  $N = (N_1 + N_2 + N_3)$ . By collocating at the same set of nodal points  $(x_i, y_i)_{i=1}^N$  from the sets  $X_1$ ,  $X_2$  and  $X_3$ , the displacements  $u(x_i, y_i)$  and  $v(x_i, y_i)$  in equations (4) and (5) are approximated by CSRBFs  $\phi_{l,k}(r)$  at these collocation points. The numerical algorithm is constructed based on a simple Wendland's function  $\phi_{4,2}(r/\delta) = [1 - r/\delta]_+^6 (3 + 18r/\delta + 35(r/\delta)^2)$ . The CSRBFs interpolant for functions  $u(x_i, y_i)$  and  $v(x_i, y_i)$  are given by

$$u_h(x_i, y_i) = \sum_{j=1}^N \alpha_j \left[ [1 - r/\delta]_+^6 (3 + 18r/\delta + 35(r/\delta)^2) \right], \quad (8)$$

$$v_h(x_i, y_i) = \sum_{j=1}^N \beta_j \left[ [1 - r/\delta]_+^6 (3 + 18r/\delta + 35(r/\delta)^2) \right], \quad (9)$$

where  $r_j = \sqrt{(x_i - x_j)^2 + (y_i - y_j)^2}$  and  $\delta_j$  is a desired scaling factor. The unknown coefficients  $\beta_j$  and  $\alpha_j$  can be determined in which all the set of data points  $(x_i, y_i)_{i=1}^N \subset \mathbf{R}^2$  are distinct.

The first and second partial derivatives of equations (4) and (5) with respect to  $x$  and  $y$  can be determined by differentiating equations in (8) and (9). The approximation solutions  $u_h(x_i, y_i)$  and  $v_h(x_i, y_i)$  can be determined by substituting these partial derivatives into equations (4) and (5), which yields the following system of equations

$$\frac{1}{(1-\nu)} \sum_{j=1}^N \alpha_j [M_{x_j}] + \frac{(1+\nu)}{2(1-\nu)} \sum_{j=1}^N \beta_j [P_j] + \frac{1}{2} \sum_{j=1}^N \alpha_j [M_{y_j}] = 0 \quad (10)$$

$$\frac{1}{(1-\nu)} \sum_{j=1}^N \beta_j [M_{y_j}] + \frac{(1+\nu)}{2(1-\nu)} \sum_{j=1}^N \alpha_j [P_j] + \frac{1}{2} \sum_{j=1}^N \beta_j [M_{x_j}] = 0 \quad (11)$$

where  $M_{x_j} = \frac{\partial^2(\phi_{4,2}(r_j/\delta_j))}{\partial x^2}$ ,  $M_{y_j} = \frac{\partial^2(\phi_{4,2}(r_j/\delta_j))}{\partial y^2}$  and  $P_j = \frac{\partial^2(\phi_{4,2}(r_j/\delta_j))}{\partial x \partial y}$ . The specific boundary conditions  $\Gamma_i$ 's as described in Figure 2 are given by

	Edge crack model	Centre crack model
$\Gamma_1$ :	$\sigma_x = 0, \tau_{xy} = 0, x = -\frac{a}{2}, 0 \leq y \leq \frac{a}{2}$ ;	$u = 0, \tau_{xy} = 0, x = 0, 0 \leq y \leq \frac{a}{2}$ ;
$\Gamma_2$ :	$\sigma_x = 0, \tau_{xy} = 0, x = \frac{a}{2}, 0 \leq y \leq \frac{a}{2}$ ;	$\sigma_x = 0, \tau_{xy} = 0, x = \frac{a}{2}, 0 \leq y \leq \frac{a}{2}$ ;
$\Gamma_3$ :	$\sigma_y = 10, \tau_{xy} = 0, -\frac{a}{2} \leq x \leq \frac{a}{2}, y = \frac{a}{2}$ ;	$\sigma_y = 10, \tau_{xy} = 0, 0 \leq x \leq \frac{a}{2}, y = \frac{a}{2}$ ;
$\Gamma_4$ :	$\sigma_y = 0, \tau_{xy} = 0, -\frac{a}{2} \leq x \leq 0, y = 0$ ;	$\sigma_y = 0, \tau_{xy} = 0, 0 \leq x \leq \frac{a}{4}, y = 0$ ;
$\Gamma_5$ :	$\nu = 0, \tau_{xy} = 0, 0 \leq x \leq \frac{a}{2}, y = 0$	$\nu = 0, \tau_{xy} = 0, \frac{a}{4} \leq x \leq \frac{a}{2}, y = 0$ .

For each collocation point in  $\Omega_1 \cap \Omega_2$ , two equations would be set according to the form:  $u = u_r \cos \theta - u_\theta \sin \theta$ , and  $v = u_r \sin \theta + u_\theta \cos \theta$ , where  $u, v$  are the displacements in the  $x, y$  directions found by the radial basis function method,  $u_r, u_\theta$  are the radial and tangential displacements respectively found by the series method.

In calculating the numerical solutions in the vicinity of the crack tip we select  $N_s = (N_4 + N_5)$  distinct nodal points  $(x_k, y_k)$  in the neighbourhood of the crack tip, where  $N_4$  is a number of points in  $(\partial\Omega_1 \cap \Omega_2)$  and  $N_5$  is a number of boundary points in  $\partial\Omega_2$  for  $\theta = 0$ . The displacements of these nodal points are approximated by the series expansions (6) and (7). Since the analytic solution given by (6) and (7) automatically satisfy the equilibrium equations (4) and (5), as well as the boundary conditions for  $\theta = \pi$ , we only need to consider the remaining boundary conditions.

The present algorithm combined with least square approximation method to obtain the best fit coefficients  $C_{1i}$  and  $C_{2i}$  of the series expansions (6) and (7). In applying the least square method, we choose  $l$  extra nodal points in  $\Omega_2$ , where  $l \geq 3$ . The nodal points have a one-one correspondence between their polar coordinates and their Cartesian coordinates:  $(r_k, \theta_k) \Leftrightarrow (x_k, y_k)$ , where  $x_k = r_k \cos \theta_k$  and  $y_k = r_k \sin \theta_k$ , for  $k = 1, \dots, (N_s + l)$ . The sum of squares of the error for functions  $u$  and  $v$  are given by

$$S_1 = \sum_{(x_k, y_k)} [u_h(x_k, y_k) - (u_{r_k} \cos \theta_k - u_{\theta_k} \sin \theta_k)]^2,$$

$$S_2 = \sum_{(x_k, y_k)} [v_h(x_k, y_k) - (u_{r_k} \sin \theta_k + u_{\theta_k} \cos \theta_k)]^2,$$

where  $u_r$  and  $u_\theta$  are the series expansion defined in equations (6) and (7). The best fit coefficients  $C_{1i}$  and  $C_{2i}$ ,  $i = 1, 2, \dots, N_s$  can be determined accordingly by minimizing the sum of the squares of the error  $S_1$  and  $S_2$  by

$$\frac{\partial S_1}{\partial C_{1i}} = 0, \text{ and } \frac{\partial S_2}{\partial C_{2i}} = 0, \text{ for } i = 1, 2, \dots, N_s. \quad (12)$$

In the numerical computation, the equations (10), (11), (12) and the given boundary conditions are re-arranged to a matrix form  $[\mathbf{Q}][\mathbf{\bar{a}}] = [\mathbf{\bar{p}}]$ , where  $[\mathbf{Q}]$  has order  $2(N + N_s) \times$

$2(N + N_s)$ ,  $[\vec{\mathbf{a}}]$  and  $[\vec{\mathbf{p}}]$  are  $2(N + N_s)$  column vectors. Since CSRBF is a class of positive definite and continuously differentiable function, the resulting matrix  $[\mathbf{Q}]$  is conditionally positive definite and hence invertible. Once the unknown coefficients are determined, the approximation solutions  $u_h(x_i, y_i)$  and  $v_h(x_i, y_i)$  can be calculated accordingly by using equations (8) and (9). For the numerical comparison, we computed the mode I stress intensity factor  $K_I$  as given by  $K_I = \lim_{r \rightarrow 0} (\sqrt{2\pi r} \sigma_\theta) = \sqrt{2\pi} C_{11}$ , from the result of analysis. The numerical results of the two considered models are compared against the one listed in standard textbook [4] as shown in Table 1.

Table 1: Stress intensity factor in the vicinity of crack tip

Stress intensity factor ( $K_I$ )		
	Our Results	Textbook [4] results
Edge crack model	32.8	35.4
Centre crack model	20.8	21.0

The numerical results of  $K_I$  agree well with the well-known results, this indicates a good performance of the proposed method in applying to solve mode I crack models. The conditioning number and the computational efficient are significantly improved due to the sparse resultant matrix. The degree of accuracy of the numerical results is very much dependent on the size of the local support  $\delta_j$ . The accuracy of the computations can be enhanced by using large scaling factor  $\delta_j$  to increase the support for the function, however this results in more intensive computation.

**Acknowledgment** This research is supported by the Research and Development Fund of the Open University of Hong Kong, No. 03/1.2.

**Reference**

1. Wu, Zongmin (1995): "Positive definite radial functions with compact support", *J. Adv. in Comput. Math.* No. 4, pp. 283-292.
2. Wendland, H. (1995): "Piecewise polynomial, positive definite and compactly compacted radial functions of minimal degree", *J. Adv. in Comput. Math.* Math. No. 4, pp. 389-396.
3. Wendland, H. (1998): "Error estimates for interpolation by compactly supported radial basis functions of minimal degree", *J. Approx. Theory*, Vol. 93, No. 2, pp. 258-272.
4. John A. Nairn (2001): "Series Solution to Stresses Around Crack Tips textquotedblright, <http://www.eng.utah.edu/~nairn/classes/mse6481/Series.pdf>.
5. Budynas, Richard G. (1999): "Advance Strength and Applied Stress Analysis", *second edition, McGraw Hill, ISBN 0-07-008985-X*.